

The propagation of Love and Rayleigh waves in the Andean Region

Lawrence A. Drake and Estela Minaya Ramos
Observatorio San Calixto, La Paz, Bolivia

RESUMEN

El patrón distintivo desde la fuente sísmica de un campo irradiado de ondas sísmicas se modifica profundamente al pasar por una región irregular como la Cordillera de los Andes de América del Sur. La onda Lg guiada por la corteza es útil en la discriminación de fuentes sísmicas, pero, aun para una sola fuente, las amplitudes de ondas de período corto como Lg pueden variar significativamente. La Cordillera de los Andes de Bolivia forma una parte de la cadena de los Andes, que se originó en los dos principales ciclos orogénicos del Fanerozoico, un Ciclo Preandino Precámbrico-Paleozoico Superior y el Ciclo Andino Mesozoico-Cenozoico. Durante el último Ciclo, cuatro sistemas del arco magmático se desarrollaron sucesivamente hacia el este: un arco Jurásico-Cretácico Temprano en la Cordillera Costera de Chile, un arco Cretácico Medio en el Valle Longitudinal de Chile, un arco Cretácico Tardío-Paleogénico en la Precordillera Chilena y el arco Mioceno-Holoceno en la Cordillera Occidental (Omarini *et al.*, 1991; Dorbath *et al.*, 1993; Scheuber *et al.*, 1994). En la región del Cabalgamiento Andino Principal entre la Cordillera Oriental (o Real) y las Sierras Subandinas en Bolivia septentrional, hay superposición de aproximadamente 230 km de edad Neogena (Roeder, 1988). Las areniscas cloríticas Permianas marinas cerca de Copacabana sobre el Lago Titicaca y las diamictitas, areniscas, cuarcitas y lutitas Ordovícico-Silúricas apretadamente plegadas, expuestas abundantemente en los cortes del camino entre Cochabamba y Caracollo, se encuentran a elevaciones desde 3800 m a 4500 m sobre el nivel del mar. El sistema de fallas de la Cordillera Real, en el borde sudoccidental, marca un límite subvertical, con buzamiento al sudoeste, que separa dos unidades de velocidad contrastante hasta una profundidad de 140 km. La profundidad al Moho debajo del Altiplano fue encontrada por Dorbath *et al.* (1993) aproximadamente a 60 km y, debajo de la Cordillera Real, aproximadamente a 50 km. Más al sur, a través del Sur de Bolivia y Norte de la Argentina, Wigger *et al.* (1994) encontraron que la profundidad al Moho debajo del Altiplano es aproximadamente de 72 km y, debajo de la Cordillera Real aproximadamente a 65 km. La propagación de las ondas de Love y de Rayleigh de período corto, a lo largo de un perfil que atraviesa estas unidades del Altiplano y de la Cordillera Real de Bolivia septentrional, ha sido analizada por el método de elementos finitos. Un resultado preliminar es que, sin tener en cuenta la absorción, a un período de 2 s, 91.69% de la energía del modo fundamental de la onda Love y 98.60% de la energía del modo fundamental de la onda Rayleigh son transmitidos.

PALABRAS CLAVE: Cordillera de los Andes, onda Love, onda Rayleigh.

ABSTRACT

The distinctive pattern from the seismic source of a radiated seismic wavefield is profoundly modified on passing through an irregular region like the Andean Cordillera of South America. The crustally guided wave Lg is useful in the discrimination of seismic sources, but, even from a single source, amplitude ratios of short period waves like Lg can vary significantly. The Bolivian Andean Cordillera forms part of the Andean chain, which originated in two major orogenic cycles of the Phanerozoic, a Late Precambrian-Paleozoic Preandean Cycle and the Mesozoic-Cenozoic Andean Cycle. During the latter Cycle, four magmatic arc systems developed successively eastward: a Jurassic-Early Cretaceous arc in the Coastal Cordillera of Chile, a Mid-Cretaceous arc in the Longitudinal Valley of Chile, a Late Cretaceous-Paleogene arc in the Chilean Precordillera and the Miocene-Holocene arc in the Western Cordillera (Omarini *et al.*, 1991; Dorbath *et al.*, 1993; Scheuber *et al.*, 1994). In the region of the low angle Main Andean Thrust, between the Eastern Cordillera (Cordillera Real) and the Subandean Ranges in northern Bolivia, there is overlap of approximately 230 km of Neogene age (Roeder, 1988). This contributes to keeping the conspicuous chloritic Permian marine sandstones near Copacabana on Lake Titicaca and the tightly folded Ordovician-Silurian diamictites, sandstones, quartzites and lutites, exposed abundantly in road cuts between Cochabamba and Caracollo, at elevations of from 3800 m to 4500 m above sea level. The Cordillera Real fault system, at the southwestern border of the Cordillera Real, marks a subvertical boundary, dipping to the southwest, which, from the surface down to a depth of 140 km, separates two strongly contrasting velocity units. The depth to the Moho below the Altiplano was found by Dorbath *et al.*, (1993) to be approximately 60 km and, below the Cordillera Real, to be approximately 50 km. Further south, across southern Bolivia and northern Argentina, Wigger *et al.*, (1994) found that the depth to the Moho below the Altiplano is approximately 72 km and, below the Cordillera Real, is approximately 65 km. The propagation of short period Love and Rayleigh waves along a profile crossing these vertically contrasting velocity units of the Altiplano and Cordillera Real in northern Bolivia has been analyzed by the finite element method. A preliminary result is that, without allowance for absorption, at a period of 2 s, 91.69 percent of the energy of the fundamental Love mode and 98.60 percent of the energy of the fundamental Rayleigh mode are transmitted.

KEY WORDS: Andean Cordillera, Love wave, Rayleigh wave.

INTRODUCTION

A seismic source imposes a distinctive pattern on the radiated seismic wavefield, but this pattern is profoundly

modified on passing through an irregular region like the Andean Cordillera of South America. The crustally guided wave Lg is useful in the discrimination of seismic sources, but, even from a single source, amplitude ratios of short

period waves like Lg can vary significantly (Kennett, 1993). Whitman *et al.* (1992) have noted that for a portable seismic network deployed in Jujuy Province (24°S, 65°W), Argentina, P and S waves of short period propagate beneath the plateau much more efficiently from the north and northwest than from the west and south; likewise, Sn phases from regional crustal earthquakes in the Subandean foreland fold-thrust belt to the north propagate efficiently to the Jujuy network, while Sn is not observed from foreland earthquakes located at similar distances to the south of the network. Whitman *et al.* (1992) suggest that, south of approximately 22°S, the upper mantle beneath the plateau and its adjacent foreland is more highly attenuating than the upper mantle further north. Similarly, Minaya *et al.* (1989) and Ayala (1992) have observed that, at the World-Wide Standard Seismograph Network station at La Paz, Bolivia (LPB; 16°32'S, 68°06'W; 3292 m), there is much greater attenuation of Lg waves of periods of approximately 1.2 s from the Western Cordillera to the west of La Paz than from the Brazilian and Guyana Shields to the east. Minaya *et al.* (1989) give an Lg/P ratio for earthquakes in Colombia of 2.77, decreasing to the west; this ratio for Brazil is 5.2 and for Venezuela is 4.5. Ayala (1992) gives different formulas for Lg equivalent body wave magnitude and different exponential decays of the maximum amplitude of the Lg waves with distance (0.2/degree from the west, and 0.09/degree from the east; periods were of approximately 1 to 1.5 s). The region of the Western Cordillera appears to be highly attenuating at these short periods.

We have begun to examine this irregular absorption in the Andean region of South America by analysing the propagation of Love and Rayleigh waves of short period (0.7 s to 7 s) by use of the finite element method in two dimensions in the frequency domain (Lysmer and Drake, 1972; Drake and Bold, 1989). Because we need eight or 10 elements per wavelength of these surface waves, we need models of large numbers of finite elements to represent irregular regions at short periods, and, in addition, the analysis of Rayleigh waves requires more than four times as much computer memory and computer time as the analysis of Love waves. In this finite element method of analysis, the base of the model is fixed at a depth several times the largest wavelength considered. The input to the model is a Love or Rayleigh mode (or linear combination of Love or Rayleigh modes); the output gives the amplitudes and phases of the resulting reflected and transmitted modes, from which phase velocities across the model and reflected and transmitted displacements or energies can be readily computed. In this paper we present very briefly results at a period of 2 s of the propagation of the fundamental Love and Rayleigh modes across a finite element model of 40 rows and 100 columns, of depth 73.8 km below the Altiplano and 75.8 km below the Cordillera Real (i.e. 70 km below sea level) and of width 62 km. For this initial presentation, we did not include the absorption of the model, in order to check that the sum of the reflected and transmitted energies of the Love and Rayleigh modes exactly balanced the incident energies. Strictly, the raised block to the northeast and east of the Altiplano in Bolivia is the Cordillera Real (16°S, 68°W; 20°S, 65°W; Ahlfeld,

1972, pp. 19-20). The Cordillera Oriental, reaching an altitude of 5200 m, is a little to the northeast of the Cordillera Real and just north and northeast of the city of Cochabamba (17°24'S, 66°09'W). However, the term "Eastern Cordillera" usually refers to the Cordillera Real (Figure 1).

TECTONIC SETTING

Isacks (1988), Ayala (1991), Dewey and Lamb (1992) and Cahill and Isacks (1992) have mapped the warping of the Nazca plate under South America. It appears to be approximately flat in the region of the Bucaramanga (07°08'N, 73°09'W) nest of earthquakes of intermediate depth in northern Colombia. In the volcanic region of Colombia and Ecuador from 5°N to 2°S, the three nests of earthquakes of intermediate depth (near 04°8N, 76°0W; 03°0N, 74°5W; 01°5S, 77°8W) indicate that the Nazca plate dips at angles between approximately 20° and 30°. In northern and central Peru, it flattens at a depth of about 130 km for 300 km toward the northeast and then turns down again (Dorbath *et al.*, 1990; Sébrier *et al.*, 1985; 1988; Stacey, 1992, p. 189). In southern Peru, at 15°S, there is a sharp flexure of the plate and its dip under Bolivia is approximately 30°. There is a gradual transition southward to nearly horizontal dip in the region from 28°S to 32°S beneath western Argentina. At 33°S there is another sharp flexure of the plate to a dip of approximately 30°. At 45°S there is a triple junction with the Antarctic plate. In addition, there is an 'elbow' in the Peru-Chile trench near Arica (18°29'S, 70°20'W) and this causes extreme complexity in the structure of the Cordillera Real and the Subandean Zone in central Bolivia (18°S, 66°W). Vega and Buforn (1991) and Dewey and Lamb (1992) have investigated the focal mechanisms of earthquakes in this region. As a result of the consequent 'elbow' in the Nazca plate, it spreads and there are two main bands of associated deep earthquakes, one from 06°5S, 71°5W, to 11°5S, 71°0W, in western Brazil and southern Peru, and the other from 19°0S, 63°5W, to 28°5S, 63°0W, in southern Bolivia and northern Argentina (Okal *et al.*, 1994). On 9 June 1994, a deep event that was felt as far away as Toronto in Canada occurred between these zones (Figure 1; Harvard centroid time and location, 00:33:44.4, 13°81S, 67°20W, depth 657.4 km; Mw 8.3).

The Bolivian Andean Cordillera forms part of the Andean chain, which originated in two major orogenic cycles of the Phanerozoic, the Late Precambrian-Paleozoic Preandean Cycle and the Mesozoic-Cenozoic Andean Cycle (Omarini *et al.*, 1991; Dorbath *et al.*, 1993; Scheuber *et al.*, 1994). During the Preandean Cycle, huge deposits developed successively further westward, from the Subandean Ranges in Bolivia and northern Argentina to the Longitudinal Valley and Coastal Cordillera in Chile. During the Andean Cycle, four magmatic arc systems developed successively eastward: a Jurassic-Early Cretaceous arc in the Coastal Cordillera of Chile, a Mid-Cretaceous-Paleogene arc in the Chilean Precordillera and the Miocene-Holocene arc in the Western Cordillera (Figure 1; Castañón and Rodrigo, 1978, p. 41; Instituto Geográfico Militar, 1985, p. 166; Ahlfeld, 1972, p. 40). In the region of the

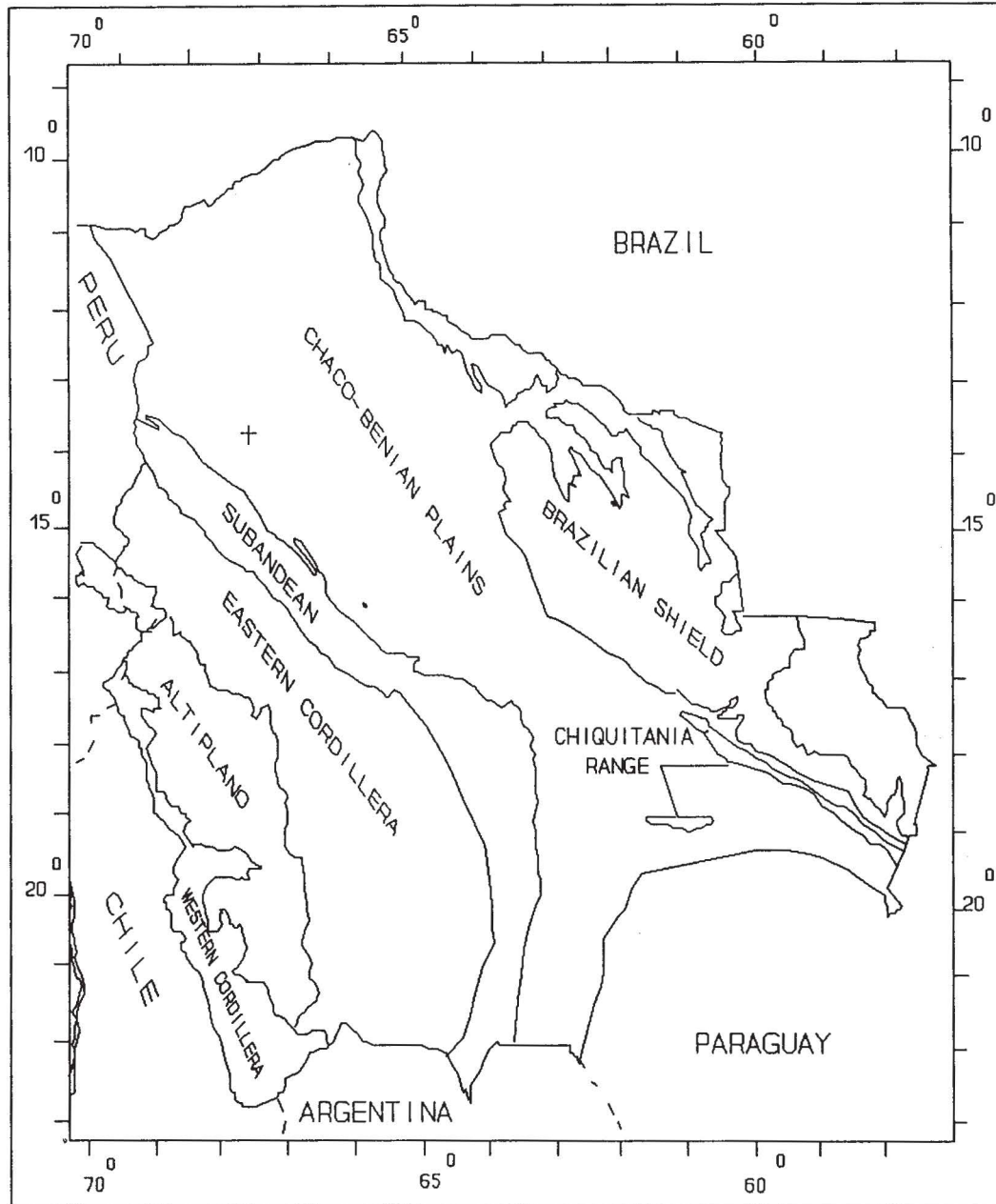


Fig. 1. Morphological zoning of the Central Andes in the region of Bolivia. The cross marks the moment centre of the deep earthquake of 9 June 1994 ($13^{\circ}.81S$, $67^{\circ}.20W$). The two-dimensional finite element section extended 62 km northeast from $17^{\circ}S$, $68^{\circ}W$, being approximately centered on the Cordillera Real fault system.

low angle Main Andean Thrust, between the Cordillera Real and the Subandean Ranges in northern Bolivia, there is overlap of approximately 230 km of Neogene age (23 Ma; 1 cm/year; Figure 2; Nevado Sajama is at $18^{\circ}06'S$, $68^{\circ}54'W$; Dorbath *et al.*, 1993; Roeder, 1988). Allmendinger *et al.* (1990) describe a similar overlap in Argentina at latitude $30^{\circ}S$. This overlap in northern and central Bolivia contributes to keeping the conspicuous chloritic Permian marine sandstones near Copacabana on Lake Titicaca (Ahlfeld, 1972, p. 64) and the tightly folded Ordovician-Silurian diamictites, sandstones, quartzites and lutites, exposed abundantly in road cuts between Cochabamba and Caracollo (Instituto Geográfico Militar, 1985,

p. 166), at elevations of from 3800 m to 4500 m above sea level. The widespread Cretaceous marine El Molino Formation in the Altiplano and Cordillera Real (Ahlfeld, 1972, p. 72; Riccardi, 1988, p. 38) indicates that this uplift has taken place since the Cretaceous; the present uplift rate of the Altiplano is 1 mm/y (Dewey and Lamb, 1992).

The Cordillera Real fault system, at the southwestern border of the Cordillera Real, marks a subvertical boundary, dipping to the southwest; from the surface down to a depth of 140 km, it separates two strongly contrasting velocity units (Dorbath *et al.*, 1993). The depth to the Moho below the Altiplano was found by these authors to be ap-

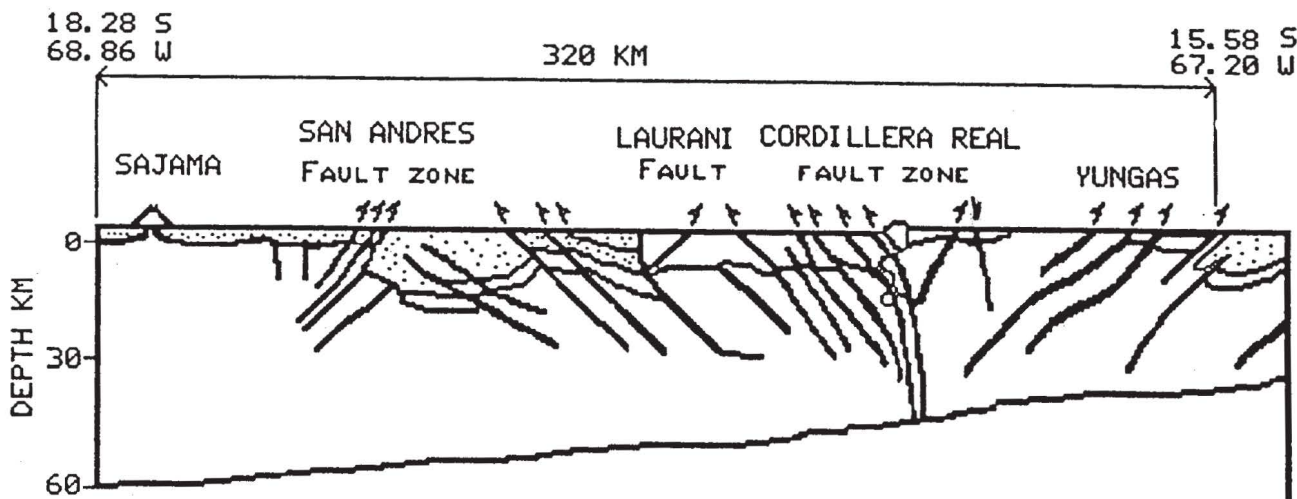


Fig. 2. Geological and structural cross section northeast from Nevado Sajama (18°06'S, 68°54'W; after Dorbath *et al.*, 1993).

proximately 60 km and, below the Cordillera Real, to be approximately 50 km. Further south, across southern Bolivia and northern Argentina, Wigger *et al.* (1994) found that the depth to the Moho below the Altiplano is approximately 72 km and, below the Cordillera Real, is approximately 65 km. Since Dorbath *et al.* interpreted P-wave arrival time residuals solely as velocity variations, their depths to the Moho under the Altiplano and Cordillera Real are not well constrained. James (1971) estimated that the depth to the Moho beneath the Altiplano is approximately 70 km and, beneath the Cordillera Real, is approximately 60 km (cf. Ocola *et al.*, 1971; Wigger *et al.*, 1991; Beck *et al.*, 1994a; 1994b). The Brazilian Shield under the Cordillera Real appears to be partially molten (Wigger *et al.*, 1994; Giese, 1994). Measurements of (primordial) mantle. ^3He indicate active mantle melting under the Cordillera Real (Hoke *et al.*, 1994). Surprisingly, with 230 km of thrusting, there is normal faulting in the western part of the Cordillera Real (Figure 2; Dorbath *et al.*, 1993). The explanation appears to be that the Brazilian Shield is causing a vertical gravitational stress with a corresponding horizontal extension. Schwartz (1988) has offered this explanation for the spectacular normal faulting (e.g. 3 m in the Ancash earthquake of 1946) in the Cordillera Blanca Fault Zone in the northern Peruvian Andes (cf. Sébrier, 1985; 1988; Suárez *et al.*, 1983).

In western Bolivia, southeast of Lake Titicaca, there is left-hand strike-slip on the Laurani fault (Dorbath *et al.*, 1993), but in central Bolivia, southeast of Cochabamba, there is right-hand strike-slip on, for example, the north-south Aiquile fault (18°S, 65°15'W; Vega and Buform, 1991; Dewey and Lamb, 1992). The brief explanation of this difference is that the pole of rotation of the Nazca-South America plate convergence is at 56°N, 94°W (Fowler, 1990, p. 13; Gordon, 1995); the resulting convergence at Arica (18°29'S, 70°20'W) is 8.24 cm/y with an azimuth of 77°; the resulting principal compressive stress from the Nazca plate on the Andes, striking NW-SE in the region of the Laurani fault, is towards the right along the

strike of the fault and this causes left-hand strike-slip; in the region of the Aiquile fault, the strike of the Andes is N-S; the resulting principal compressive stress is towards the left along the strike of the fault and this causes right-hand strike-slip.

A TWO-DIMENSIONAL FINITE ELEMENT MODEL

A two-dimensional section of this highly irregular and deforming region, along a part of the profile of length 320 km of Dorbath *et al.* (1993), northeast from the region of Nevado Sajama and passing just southeast of La Paz, has been modelled by the finite element method. The section of the finite element model was in a northeast direction from 17°S, 68°W, near the half-way mark of the profile of Dorbath *et al.* (1993). The length of the finite element model was 62 km and it was centered at the Cordillera Real fault system, between the Altiplano and the Cordillera Real. The depth of the finite element model was 73.8 km below the Altiplano and 75.8 km below the Cordillera Real. The horizontally layered structures representing the region of the Altiplano to a depth of 73.8 km are shown in Tables 1 and 2 (Wigger *et al.*, 1991; 1994; Dorbath *et al.*, 1993). Values of Poisson's ratio and the properties of the earth's mantle were taken from global models (Dziewonski and Anderson, 1981; Dziewonski *et al.*, 1975; Morelli and Dziewonski, 1993; Kennett, 1995). The normalized variation with depth of the displacement of the fundamental Love mode at periods of 3.5 s and 2.0 s for the regions of the Cordillera Real and of the Altiplano is tabulated in Table 3 and shown in Figure 3. The modes are normalized such that the energy they transport is proportional to the product of their wave number, their frequency and the square of their amplitude (Lysmer and Drake, 1972). The normalized variation with depth of the horizontal and vertical displacements of the fundamental Rayleigh mode at a period of 3.5 s for the regions of the Cordillera Real and the Altiplano is tabulated in Table 4 and shown in Figure 4.

LOVE WAVE DISPLACEMENT DEPTH VARIATION, 3.5, 2 S

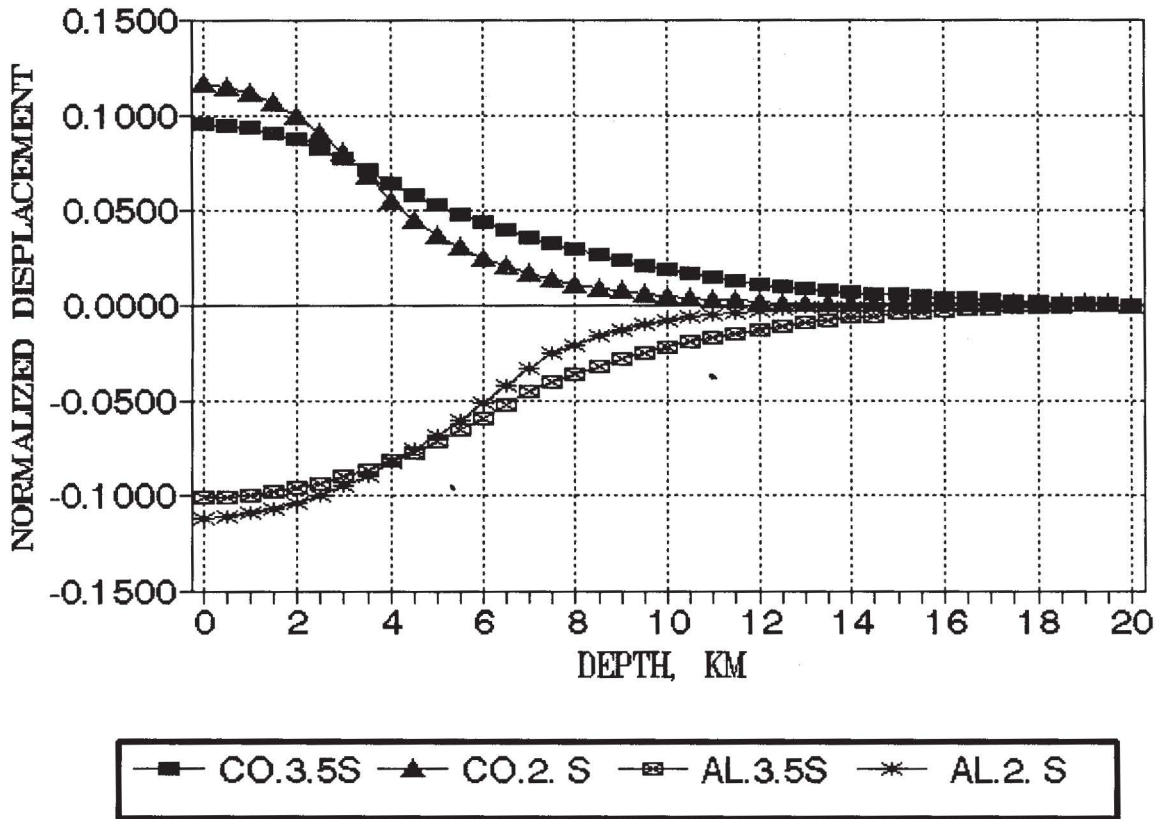


Fig. 3. Normalized variation with depth of the displacement of the fundamental Love mode at periods of 3.5 s and 2.5 s for the regions of the Cordillera Real and the Altiplano.

Table 1

Model of the Altiplano region to a depth of 73.8 km.

Layer thickness km	Compressional velocity km/s	Shear velocity km/s	Density g/cm ³	Poisson's ratio	Quality factor Q
7.0	4.50	2.70	2.50	0.219	20
7.0	5.00	2.97	2.70	0.227	30
6.0	5.40	3.21	2.70	0.227	40
8.0	6.10	3.52	2.75	0.250	60
15.8	6.20	3.58	2.75	0.250	80
6.0	6.50	3.75	2.83	0.251	100
6.0	5.90	3.41	2.83	0.249	50
6.0	6.50	3.75	2.95	0.251	200
12.0	8.10	4.74	3.24	0.240	400

The upper central section (of width 50.8 km) of the two-dimensional finite element model of the region from the Altiplano to the Cordillera Real is shown in Figure 5. The thicknesses and material properties of the intermediate

elements of the model were averaged from the thicknesses and material properties of the layers of the end structures (of the Altiplano and the Cordillera Real). The compressional velocity, shear velocity and density are shown for

RAYLEIGH WAVE DISPLACEMENT VARIATION WITH DEPTH, 3.5 S

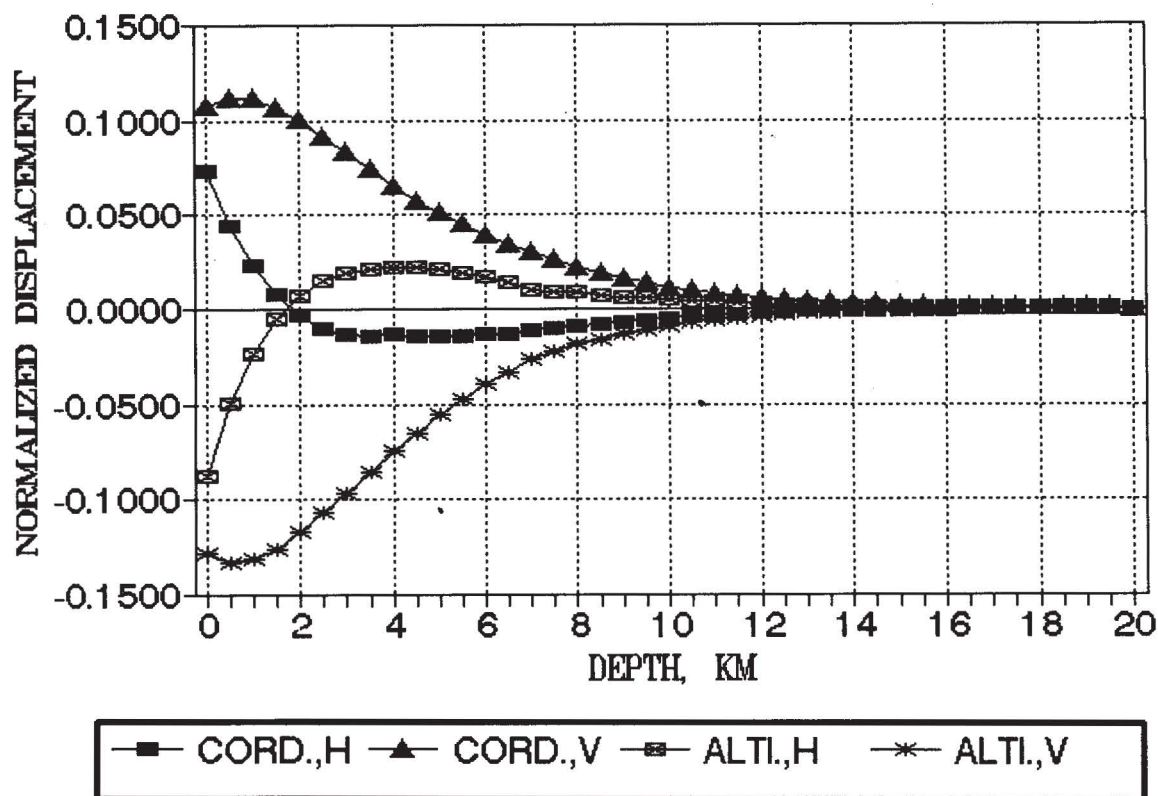


Fig. 4. Normalized variation with depth of the horizontal and vertical displacements of the fundamental Rayleigh mode at a period of 3.5 s for the regions of the Cordillera Real and the Altiplano.

Table 2

Model of the Cordillera Real to a depth of 75.8 km.

Layer thickness km	Compressional velocity km/s	Shear velocity km/s	Density g/cm ³	Poisson's ratio	Quality factor Q
4.0	5.00	2.97	2.70	0.227	30
7.0	5.60	3.33	2.70	0.227	40
11.0	6.00	3.51	2.75	0.240	50
8.0	6.10	3.52	2.75	0.250	60
7.8	6.20	3.58	2.75	0.250	80
6.0	6.50	3.75	2.83	0.251	100
6.0	5.90	3.41	2.83	0.249	50
6.0	6.50	3.75	2.95	0.251	200
20.0	8.10	4.74	3.24	0.240	400

each section of the finite element model. The central sloping section of the model goes from a distance of 15.5 km to a distance of 46.5 km in the model of total length 62 km.

The analysis of the finite element model gives the

phase changes of the Love and Rayleigh modes of different frequencies across the irregular part of the model, and, hence, the average phase velocities of these modes within the model. Results for the fundamental Love mode and for the fundamental Rayleigh mode at a period of 2 s are tabu-

Table 3

Depth km	Normalized variation with depth of fundamental Love mode			
	Cordillera Real		Altiplano	
	3.5 s	2.0 s	3.5 s	2.0 s
.0	.09532	.11590	-.10131	-.11172
.5	.09480	.11485	-.10099	-.11126
1.0	.09325	.11173	-.10007	-.10989
1.5	.09068	.10659	-.09852	-.10760
2.0	.08713	.09953	-.09637	-.10443
2.5	.08262	.09066	-.09364	-.10040
3.0	.07722	.08016	-.09032	-.09554
3.5	.07098	.06821	-.08646	-.08989
4.0	.06396	.05503	-.08206	-.08350
4.5	.05833	.04513	-.07716	-.07643
5.0	.05316	.03700	-.07179	-.06872
5.5	.04840	.03033	-.06597	-.06045
6.0	.04402	.02486	-.05975	-.05168
6.5	.03997	.02036	-.05317	-.04248
7.0	.03624	.01666	-.04626	-.03293
7.5	.03280	.01362	-.04115	-.02628
8.0	.02960	.01111	-.03658	-.02098
8.5	.02664	.00904	-.03248	-.01674
9.0	.02389	.00733	-.02881	-.01335
9.5	.02132	.00591	-.02551	-.01064
10.0	.01892	.00471	-.02255	-.00848
10.5	.01666	.00371	-.01989	-.00675
11.0	.01453	.00285	-.01748	-.00536
11.5	.01281	.00222	-.01530	-.00424
12.0	.01128	.00173	-.01333	-.00334
12.5	.00992	.00135	-.01152	-.00261
13.0	.00872	.00105	-.00987	-.00201
13.5	.00764	.00082	-.00835	-.00151
14.0	.00668	.00064	-.00693	-.00110
14.5	.00581	.00050	-.00585	-.00081
15.0	.00504	.00039	-.00492	-.00060
15.5	.00434	.00030	-.00412	-.00044
16.0	.00371	.00023	-.00342	-.00032
16.5	.00313	.00018	-.00282	-.00024
17.0	.00260	.00014	-.00229	-.00017
17.5	.00211	.00010	-.00183	-.00013
18.0	.00165	.00008	-.00141	-.00009
18.5	.00122	.00005	-.00102	-.00006
19.0	.00080	.00003	-.00067	-.00004
19.5	.00040	.00002	-.00033	-.00002
20.0	.00000	.00000	.00000	.00000

lated in Table 5. For the Love mode the average phase velocity within the model is 1.43 percent greater than the mean of the phase velocities in the Altiplano and the Cordillera Real. For the Rayleigh mode the average phase velocity within the model is 2.70 percent greater than the mean of the phase velocities in the Altiplano and the Cordillera Real. These results were obtained without allowance for absorption, which, in moderate amounts in fi-

nite element models, does not significantly alter phase velocities.

The analysis of the finite element model also gives the changes of amplitude of the modes across the model and the percentages of energy either retained in the modes or reflected and scattered into other modes. The changes of amplitude of the fundamental Love mode and of the fundamen-

Table 4

Depth km	Normalized variation with depth of fundamental Rayleigh mode			
	Cordillera Real		Altiplano	
	Horizontal	Vertical	Horizontal	Vertical
.0	.07324	.10784	-.08813	-.12856
.5	.04415	.11182	-.04966	-.13347
1.0	.02279	.11096	-.02306	-.13179
1.5	.00744	.10667	-.00502	-.12587
2.0	-.00320	.10002	.00690	-.11737
2.5	-.01005	.09187	.01446	-.10743
3.0	-.01375	.08289	.01894	-.09685
3.5	-.01473	.07367	.02125	-.08616
4.0	-.01317	.06471	.02204	-.07571
4.5	-.01447	.05769	.02174	-.06572
5.0	-.01480	.05105	.02065	-.05635
5.5	-.01450	.04488	.01893	-.04770
6.0	-.01380	.03923	.01662	-.03985
6.5	-.01286	.03412	.01369	-.03287
7.0	-.01181	.02954	.01000	-.02688
7.5	-.01070	.02545	.00903	-.02277
8.0	-.00961	.02182	.00803	-.01920
8.5	-.00854	.01863	.00704	-.01612
9.0	-.00752	.01581	.00612	-.01348
9.5	-.00655	.01335	.00527	-.01124
10.0	-.00562	.01121	.00452	-.00933
10.5	-.00471	.00936	.00385	-.00772
11.0	-.00379	.00779	.00327	-.00635
11.5	-.00328	.00658	.00276	-.00520
12.0	-.00283	.00554	.00232	-.00423
12.5	-.00243	.00465	.00193	-.00342
13.0	-.00208	.00390	.00158	-.00274
13.5	-.00178	.00325	.00126	-.00217
14.0	-.00152	.00271	.00095	-.00171
14.5	-.00130	.00224	.00079	-.00137
15.0	-.00111	.00185	.00065	-.00110
15.5	-.00095	.00151	.00053	-.00087
16.0	-.00081	.00122	.00044	-.00069
16.5	-.00069	.00097	.00036	-.00053
17.0	-.00058	.00076	.00030	-.00041
17.5	-.00049	.00057	.00024	-.00030
18.0	-.00040	.00041	.00020	-.00022
18.5	-.00032	.00028	.00015	-.00014
19.0	-.00023	.00016	.00011	-.00008
19.5	-.00012	.00007	.00006	-.00003
20.0	.00000	.00000	.00000	.00000

tal Rayleigh mode at a period of 2 s are tabulated in Table 6. The surface amplitude of the fundamental Love mode actually increases by 5.09 percent on passing from the Altiplano to the Cordillera Real. Because 91.69 percent of the energy of the fundamental Love mode at a period of 2 s is transmitted from the Altiplano to the Cordillera Real, 8.31 percent of the energy of this mode goes into reflected and forward scattered modes. Energy in the fundamental Love

mode below the surface of the Altiplano has passed to the surface in the fundamental Love mode of the Cordillera Real to give the increase of surface amplitude. It is surprising that the surface amplitude of the fundamental Love wave increases on passing from the 20 km thickness of sediments of the Altiplano to the rock of the Cordillera Real. Allowance for absorption will partially resolve this problem. The horizontal surface amplitude of the funda-

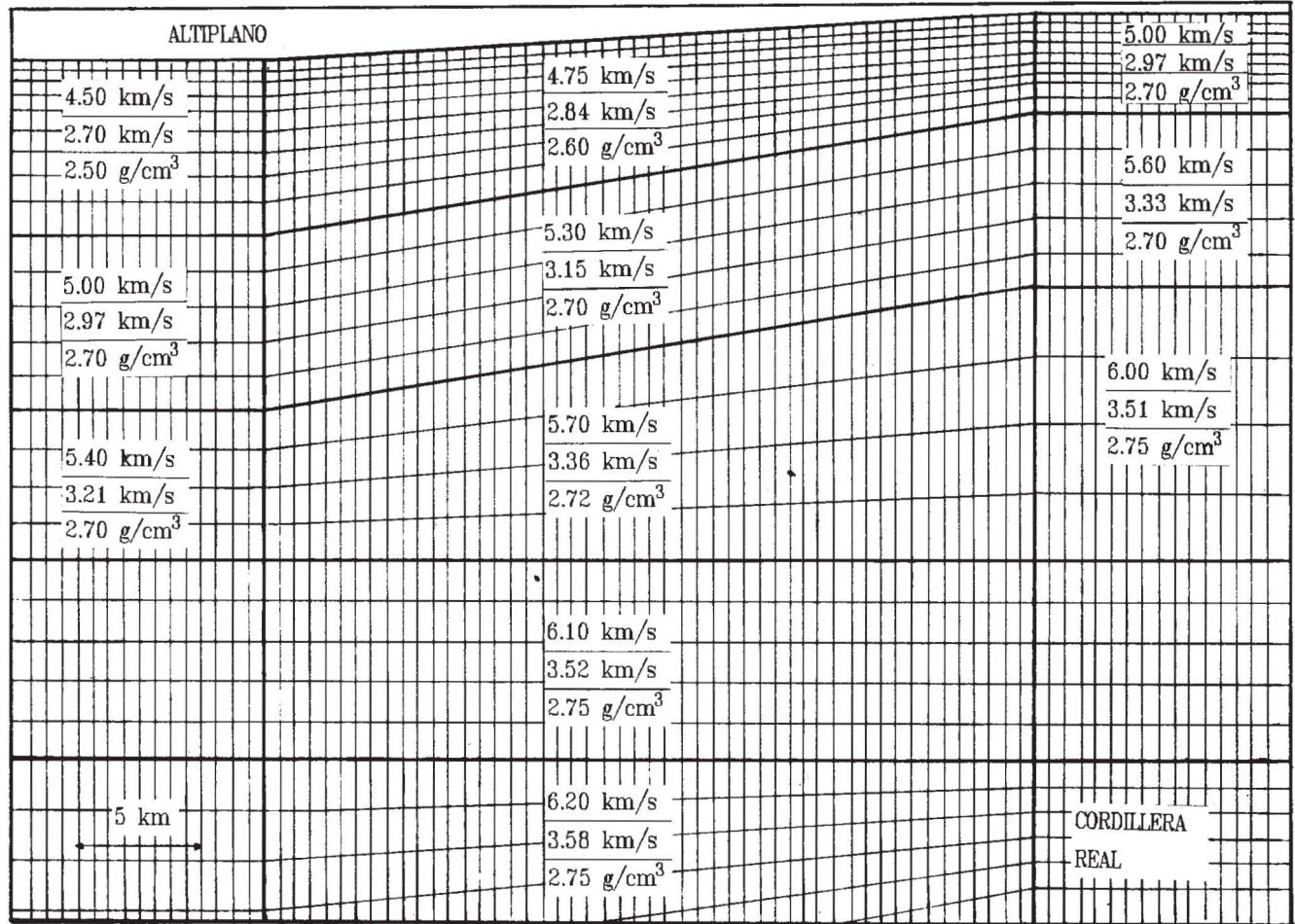


Fig. 5. Upper central section (width 50.8 km) of the finite element model of the region from the Altiplano of northern Bolivia to the Cordillera Real. The central sloping section goes from a distance of 15.5 km to a distance of 46.5 km in the finite element model of total width 62 km.

Table 5

Phase velocities from the Altiplano to the Cordillera Real.

Phase velocity km/s	Altiplano	Transition zone	Cordillera Real
Love wave	2.7337	2.9441	3.0717
Rayleigh wave	2.4805	2.6905	2.7590

Table 6

Displacements from the Altiplano to the Cordillera Real.

Surface displacement	Altiplano	Cordillera Real
Love wave	0.1119	0.1176
Rayleigh wave: horizontal	0.1104	0.0998
Rayleigh wave: vertical	0.1620	0.1478

mental Rayleigh mode decreases by 9.60 percent on passing from the Altiplano to the Cordillera Real, and the vertical surface amplitude decreases by 8.77 percent. Allowance for absorption will obviously make these decreases greater. Because 98.60 percent of the energy of the fundamental Rayleigh mode passes from the Altiplano to the Cordillera Real, only 1.40 percent of the energy of this mode is reflected and scattered.

Absorption of Lg in the Western Cordillera is probably connected with the high heat flow (80 mW/m²) and the volcanism there since the beginning of the Neogene. Heat flow in the Cordillera Real is less (60 mW/m²; Omarini *et al.*, 1991; Giese, 1994). Besides the model of the transition between the Altiplano and the Cordillera Real, we have constructed two-dimensional finite element models of the trench and coast of Chile (southwest of La Paz), of the northern coast of Colombia (northnorthwest of La Paz) and of the transition between the Western Cordillera and the Altiplano. We are continuing to analyse these models, without and with allowance for absorption.

CONCLUSIONS

A seismic source imposes a distinctive pattern on the radiated seismic wavefield, but this pattern is profoundly modified on passing through an irregular region like the Andean Cordillera. Minaya *et al.* (1989) observed at La Paz, Bolivia, much greater attenuation of Lg waves of periods of approximately 1.2 s from the Western Cordillera than from the Brazilian and Guyana Shields. The Cordillera Real fault system, at the southwestern border of the Cordillera Real, marks a subvertical boundary. From the surface down to a depth of 140 km, it separates two strongly contrasting velocity units. The propagation of short period Love and Rayleigh waves along a profile crossing these vertically contrasting velocity units of the Altiplano and Cordillera Real in northern Bolivia has been analysed by the finite element method. At a period of 2 s, without allowance for absorption, the average phase velocity of the fundamental Love mode across the finite element model is 1.43 percent greater than the mean of the phase velocities in the Altiplano and the Cordillera Real. For the fundamental Rayleigh mode the average phase velocity within the model is 2.70 percent greater than the mean of the phase velocities in the Altiplano and the Cordillera Real. The surface amplitude of the fundamental Love mode actually increases by 5.09 percent on passing from the Altiplano to the Cordillera Real. Allowance for absorption will partially resolve this problem. The percentage of the energy of the fundamental Love mode transmitted is 91.69. The horizontal surface amplitude of the fundamental Rayleigh mode decreases by 9.60 percent on passing from the Altiplano to the Cordillera Real, and the vertical surface amplitude decreases by 8.77 percent. Allowance for absorption will obviously make these decreases greater. The percentage of the energy of the fundamental Rayleigh mode transmitted is 98.60. We are continuing to analyse by the finite element method in the frequency domain the propagation of Love and Rayleigh waves, without and with allowance for absorption, in models of the transition between the Altiplano and the Cordillera Real, of the coasts of Chile and northern Colombia and of the transition between the Western Cordillera and the Altiplano in northern Chile and Bolivia.

ACKNOWLEDGEMENTS

Research sponsored by the Air Force Office of Scientific Research, Air Force Material Command, USAF, under Grant Number F49620-93-1-0433. The U.S. Government is authorized to reproduce and distribute reprints for Governmental purposes notwithstanding any copyright notation thereon.

The views and conclusions contained in this document are those of the authors and should not be interpreted as necessarily representing the official policies, either express or implied, of the Air Force Office of Scientific Research or the U.S. Government.

BIBLIOGRAPHY

- AHLFELD, F. E., 1972. Geología de Bolivia. Amigos del Libro, Cochabamba, 191 pp.
- ALLMENDINGER, R.W., D. FIGUEROA, D. SNYDER, J. BEER, C. MPODOZIS and B. L. ISACKS, 1990. Foreland shortening and crustal balancing in the Andes at 30°S latitude. *Tectonics*, 9, 789-809.
- AYALA, R. R., 1991. Deriva continental y tectónica de placas con relación a la evolución de la placa de Nazca y los Andes Centrales. *Revista: Academia Nacional de Ciencias*, 6, 98-118. (Bolivia).
- AYALA, R. R., 1992. Magnitud m_{bLg} para sismos sudamericanos. *Revista Geofísica, Instituto Panamericano de Geografía e Historia*, 36, 123-134.
- BECK, S., T. WALLACE, S. MYERS, J. SWENSON, M. TINKER, R. BRAZIER, P. SILVER, R. KUEHNEL, L. A. DRAKE, E. MINAYA, R. ALCALA, P. SOLER, P. BABY, B. GUILLER, G. ZANDT, D. ROCK, S. RUPPERT, J. TELLERIA and S. BARRIENTOS, 1994a. A passive broadband seismic experiment in the Central Andean Cordillera: the BANJO and SEDA experiments. Asamblea Regional de Sismología en América del Sur, Brasilia, Brasil, Abstracts, p. 73.
- BECK, S., P. SILVER, G. ZANDT, T. WALLACE, S. MYERS, R. KUEHNEL, S. RUPPERT, L. A. DRAKE, E. MINAYA, P. SOLER, P. BABY, S. BARRIENTOS, J. TELLERIA, M. TINKER and J. SWENSON, 1994b. Across the Andes and along the Altiplano: a passive seismic experiment. *IRIS Newsletter*, 13, No. 3, 1-3.
- CAHILL, T. and B. L. ISACKS, 1992. Seismicity and shape of the subducted Nazca plate. *J. Geophys. Res.*, 97, 17, 503-17, 529.
- CASTAÑOS, A. and L. A. RODRIGO, 1978. Sinopsis estratigráfica de Bolivia: Parte de Paleozoico. Academia Nacional de Ciencias de Bolivia, La Paz, 152 pp.
- DEWEY, J. F. and S. H. LAMB, 1992. Active tectonics of the Andes. *Tectonophysics*, 205, 79-95.
- DORBATH, L., A. CISTERNAS and C. DORBATH, 1990. Assessment of the size of large and great historical earthquakes in Peru. *Bull. Seism. Soc. Am.*, 80, 551-576.
- DORBATH, C., M. GRANET, G. POUPINET and C. MARTINEZ, 1993. A teleseismic study of the Altiplano and the Eastern Cordillera in northern Bolivia: new constraints on a lithospheric model. *J. Geophys. Res.*, 98, 9825-9844.
- DRAKE, L. A., and B. A. BOLT, 1989. Finite element modelling of surface wave transmission across regions of subduction. *Geophys. J. Int.*, 98, 271-279.

- DZIEWONSKI, A. M. and D. L. ANDERSON, 1981. Preliminary Earth reference model. *Phys. Earth Planet. Interiors*, 25, 297-359.
- DZIEWONSKI, A. M., A. L. HALES and E. R. LAPWOOD, 1975. Parametrically simple Earth models consistent with geophysical data. *Phys. Earth. Planet. Interiors*, 10, 12-48.
- FOWLER, C. M. R., 1990. *The Solid Earth*. Cambridge University Press, Cambridge, 490 pp.
- GIESE, P., 1994. Geothermal structure of the central Andean crust-implications for heat transport and rheology. In: K.-J. Reutter, E. Scheuber and P. J. Wigger (Editors), *Tectonics of the Southern Central Andes*. Springer-Verlag, Berlin, pp. 69-76.
- GORDON, R. G., 1995. Present plate motions and plate boundaries. In: T. J. Ahrens (Editor), *Global Earth Geophysics: a Handbook of Physical Constants*. American Geophysical Union, Washington, pp. 66-87.
- HOKÉ, L., D. R. HILTON, S. H. LAMB, K. HAMMERSCHMIDT and H. FRIEDRICHSEN, 1994. The evidence for a wide zone of active mantle melting beneath the Central Andes. *Earth Planet. Sci. Lett.*, 128, 341-355.
- INSTITUTO GEOGRAFICO MILITAR, 1985. *Atlas de Bolivia*. Geomundo, Barcelona, 216 pp.
- ISACKS, B. L., 1988. Uplift of the Central Andean Plateau and bending of the Bolivian Orocline. *J. Geophys. Res.*, 93, 3211-3231.
- JAMES, D. E., 1971. Andean crustal and upper mantle structure. *J. Geophys. Res.*, 76, 3246-3271.
- KENNETT, B. L. N., 1993. The distance dependence of regional phase discriminants. *Bull. Seism. Soc. Am.*, 83, 1155-1166.
- KENNETT, B. L. N., 1995. Seismic traveltimes tables. In: T. J. Ahrens (Editor), *Global Earth Geophysics: a Handbook of Physical Constants*. American Geophysical Union, Washington, pp. 126-143.
- LYSMER, J. and L. A. DRAKE, 1972. A finite element method for seismology. In: B. A. Bolt (Editor), *Methods in Computational Physics*. Academic Press, New York, pp. 181-216.
- MINAYA, E., R. R. AYALA, I. ALCOCER and R. CABRE, 1989. Ondas Lg de sismos sudamericanos. *Revista Geofísica, Instituto Panamericano de Geografía e Historia*, 31, 115-146.
- MORELLI, A. and A. M. DZIEWONSKI, 1993. Body wave traveltimes and a spherically symmetric P- and S-wave velocity model. *Geophys. J. Int.*, 112, 178-194.
- OCOLA, L.C., R.P. MEYER and L.T. ALDRICH, 1971. Gross crustal structure under Peru-Bolivia Altiplano. *Earthquake Notes*, 42 (3-4), 33-48.
- OKAL, E., S. KIRBY., E. R. ENGDAHL and W. C. HUANG, 1994. Deep earthquakes beneath South America and their physical significance. *Asamblea Regional de Sismología en América del Sur, Brasilia, Brasil (Abstracts)*, pp. 134-135.
- OMARINI, R., K. REUTTER and T. BOGDANIC, 1991. Geological development and structures. In: R. Omarini and H. J. Gotze (Editors), *Central Andean Transect, Nazca Plate to Chaco Plains: Southeastern Pacific Ocean, Northern Chile and Northern Argentina, Global Geoscience Transect 6*. American Geophysical Union, Washington, pp. 5-12.
- RICCARDI, A. C., 1988. The Cretaceous System of Southern South America. *Geol. Soc. Am. Mem.*, 168, Boulder, 166 pp.
- ROEDER, D., 1988. Andean-age structure of Eastern Cordillera (Province of La Paz, Bolivia). *Tectonics*, 7, 23-39.
- SCHEUBER, E., T. BOGDANIC, A. JENSEN and K. J. REUTTER, 1995. Tectonic development of the north Chilean Andes in relation to plate convergence and magmatism since the Jurassic. In: K.-J. Reutter, E. Scheuber and P. J. Wigger (Editors). *Tectonics of the Southern Central Andes*. Springer-Verlag, Berlin, 121-139 pp.
- SCHWARTZ, D. P., 1988. Paleoseismicity and neotectonics of the Cordillera Blanca fault zone, northern Peruvian Andes. *J. Geophys. Res.*, 93, 4712-4730.
- SEBRIER, M., J. L. MERCIER, F. MEGARD, G. LAUBACHER and E. CAREY-GAILHARDIS, 1985. Quaternary normal and reverse faulting and the state of stress in the central Andes of south Peru. *Tectonics*, 4, 739-780.
- SEBRIER, M., J. L. MERCIER, J. MACHARE, D. BONNOT, J. CABRERA and J. L. BLANC, 1988. The state of stress in an overriding plate situated above a flat slab: the Andes of central Peru. *Tectonics*, 7, 895-928.
- STACEY, F. D., 1992. *Physics of the Earth* (3rd ed). Brookfield Press, Brisbane, Australia, 526 pp.
- SUAREZ, G., P. MOLNAR and B. C. BURCHFIELD, 1983. Seismicity, fault plane solutions, depth of fault-

- ing and active tectonics of the Andes of Peru, Ecuador and southern Colombia. *J. Geophys. Res.*, 88, 10403-10428.
- VEGA, A. and E. BUFORN, 1991. Focal mechanisms of intraplate earthquakes in Bolivia, South America. *Pure and Appl. Geophys. (PAGEOPH)*, 136, 449-458.
- WHITMAN, D., B. L. ISACKS, J. L. CHATELAIN, J. M. CHIU and A. PEREZ, 1992. Attenuation of high-frequency seismic waves beneath the Central Andean Plateau. *J. Geophys. Res.*, 97, 19929-19947.
- WIGGER, P. J., M. ARANEDA, P. GIESE, W.-D. HEINSOHN, P. ROWER, M. SCHMITZ and J. VIRAMONTE, 1991. The crustal structure along the central Andean transect derived from seismic refraction investigations. *In*: R. Omarini and H.-J. Gotze (Editors), Central Andean Transect, Nazca Plate to Chaco Plains: Southeastern Pacific Ocean, Northern Chile and Northern Argentina, Global Geoscience Transect 6. American Geophysical Union, Washington, pp. 13-19.
- WIGGER, P.J., M. SCHMITZ, M. ARANEDA, G. ASCH, S. BALDZUHN, P. GIESE, W.-D. HEINSOHN, E. MARTINEZ, E. RICALDI, P. ROWER and J. VIRAMONTE, 1994. Variation in the crustal structure of the southern Central Andes deduced from seismic refraction investigations. *In*: K.-J. Reutter, E. Scheuber and P.J. Wigger (Editors), Tectonics of the Southern Central Andes. Springer-Verlag, Berlin, pp. 23-48.
-
- Lawrence A. Drake and Estela Minaya Ramos
Observatorio San Calixto, Casilla 12656, La Paz, Bolivia